Acta metall. Vol. 34, No. 3, pp. 483–492, 1986
Printed in Great Britain.

0001-6160/86 $3.00 + 0.00

CHANGE OF VISCOSITY DURING STRUCTURAL RELAXATION OF AMORPHOUS $Fe_{40}Ni_{40}B_{20}$

A. VAN DEN BEUKEL, E. HUIZER, A. L. MULDER and S. VAN DER ZWAAG
Laboratory of Metallurgy, Delft University of Technology, Rotterdamseweg 137, 2628 AL Delft, The Netherlands

(*Received* 10 *January* 1985; *in revised form* 19 *June* 1985)

Abstract—Measurements of viscosity as a function of time and temperature have been carried out on amorphous $Fe_{40}Ni_{40}B_{20}$ in a temperature range where structural relaxation occurs (450–600 K). Analysis of the data shows different behaviour in two temperature ranges: (1) *Range I* (520–600 K). In this range the observed changes of viscosity can be described consistently in terms of the annealing out of flow defects (TSRO). The activation energy for motion and annihilation of the flow defects is $Q = 250$ kJ/mol. The isoconfigurational viscosity is temperature dependent according to $\eta \sim \exp(Q_\eta/RT)$ with $Q_\eta = 304$ kJ/mol. A possible explanation for the difference between Q and Q_η is proposed. (2) *Range II* (< 520 K). Here the isoconfigurational $\ln \eta$ vs T^{-1} plots yield an activation energy of about 250 kJ/mol, close to the value found for the annihilation of flow defects. The increase of viscosity observed in this range is ascribed to an increase of chemical order (CSRO). In a narrow temperature range between I and II, the contributions of TSRO and CSRO to the increase of the viscosity can be clearly distinguished.

Résumé—Nous avons effectué des mesures de viscosité en fonction du temps et de la température sur $Fe_{40}Ni_{40}B_{20}$ amorphe dans un domaine de températures où se produit la relaxation structurale (450–600 K). L'analyse des résultat permet de mettre en évidence des comportements différents dans deux domaines de températures: (1) *Domaine I* (520–600 K). Dans ce domaine, on peut décrire de manière cohérente les changements de viscosité observés par un recuit des défauts d'écoulement. L'énergie d'activation pour le mouvement et l'annihilation des défauts d'écoulement est $Q = 250$ kJ/mol. La viscosité isoconfigurationnelle dépend de la température selon $\eta \sim \exp(Q_\eta/RT)$, avec $Q_\eta = 304$ kJ/mol. Nous proposons une explication possible pour la différence entre Q et Q_η. (2) *Domaine II* (< 520 K). Ici, les tracés isoconfigurationnels de $\log \eta$ en fonction de T^{-1} conduisent à une énergie d'activation d'environ 250 kJ/mol, proche de la valeur trouvée pour l'annihilation des défauts d'écoulement. Nous attribuons l'augmentation de viscosité observée dans ce domaine à une augmentation de l'ordre chimique. Dans un étroit domaine de températures entre I et II, on peut distinguer nettement les contributions des deux mécanismes à l'augmentation de la viscosité.

Zusammenfassung—Messungen der Viskosität in Abhängigkeit von Zeit und Temperatur wurden an der amorphen Legierung $Fe_{40}Ni_{40}B_{20}$ im Temperaturbereich, in dem die strukturelle Relaxation auftritt, durchgeführt (450–600 K). Aus der Analyse ergeben sich zwei Temperaturbereiche unterschiedlichen Verhaltens: (1) *Bereich I* (520–600 *K*). Die beobachteten Änderungen in der Viskosität können konsistent mit dem Ausheilen von Fließdefekten beschrieben werden (TSRO). Die Aktivierungsenergie für Bewegung und Annihilation der Fließdefekte beträgt $Q = 250$ kJ/Mol. Die isokonfigurationelle Viskosität hängt entsprechend $\eta \sim \exp(Q_\eta/RT)$ mit $Q_\eta = 304$ kJ/Mol ab. Für den Unterschied zwischen Q und Q_η wird eine mögliche Erklärung vorgeschlagen. (2) *Bereich II* (< 520 *K*). Hier ergeben die isokonfigurationellen Auftragungen $\ln \eta$ gegen T^{-1} eine Aktivierungsenergie von etwa 250 kJ/Mol. Dieser Wert liegt nahe bei dem, der für die Annihilation der Fließdefekte gefunden worden ist. Der in diesem Bereich beobachtete Anstieg der Viskosität wird einer Zunahme der chemischen Ordnung zugeschrieben (CSRO). In einem engen Temperaturbereich zwischen den Bereichen I und II können die Beiträge von TSRO und CSRO zur Viskosität deutlich unterschieden werden.

1. INTRODUCTION

Low temperature annealing of metallic glasses causes changes in a large number of physical properties [1]. This is attributed to atomic rearrangements in the amorphous state and the term structural relaxation is generally used to indicate this process which must be clearly distinguished from crystallization.

Generally the atomic rearrangements are divided into two kinds. In the first kind only the topological atomic positions are considered regardless of the chemical species of the atoms. Changes of these topological positions e.g. the interatomic distances, are thus described in terms of topological short range order (TSRO). As a result of TSRO a.o. the density of the glass will change. In the second type of rearrangements the chemical species of the atoms is taken into account. Consequently chemical short range order (CSRO) describes changes in the local surroundings of a given atom. It is comparable to order–disorder processes in crystalline materials.

As metallic glasses are produced by rapid quenching from the melt the asquenched glass will contain a large amount of free volume and the degree of short

range order that is frozen in will be low. Structural relaxation during isothermal annealing of an as-quenched glass will result in a decrease of the amount of free volume (TSRO) and an increase of the degree of short range order (CSRO). There is a large amount of experimental evidence [1] that at suitable annealing temperatures the chemical order parameter increases to new temperature dependent equilibrium values and that subsequent annealing at higher temperatures causes a decrease in the state of local order. CSRO is therefore a reversible process. Due to the very nature of its kinetics TSRO cannot reach equilibrium under most experimental conditions before crystallization occurs. Therefore TSRO will be regarded as a non-reversible process.

In the free volume model [2, 3], expressions are given for the decay of free volume during structural relaxation. In a previous paper [4] measurements were presented of the change of length and Young's modulus during structural relaxation of $Fe_{40}Ni_{40}B_{20}$ which allowed a quantitative test of the model and a separation of the contributions of CSRO and TSRO to the property changes observed. The parameters governing the kinetics of free volume decay were derived from the experimental results. The analysis was, however, rather indirect and very complicated.

In this paper data are presented on the change of viscosity during structural relaxation of amorphous $Fe_{40}Ni_{40}B_{20}$. In the next section it is explained why the viscosity is an unique property with respect to its behaviour during structural relaxation. This makes the interpretation of the observed effects in terms of the free volume model simpler and more direct. It will be shown that the results of the analysis are in general agreement with the views presented earlier [4], whereas also some new aspects of the relaxation process are pointed out.

2. THEORY AND EXPERIMENTAL PROGRAM

In the free volume model [5] the viscosity η is given by

$$\eta = \frac{kT\Omega}{c_f k_f (\gamma_0 v_0)^2} \tag{1}$$

where c_f = concentration of flow defects = $\exp(-x^{-1})$ with $x = v_f/\gamma v^*$ v_f = free volume per atom; γv = constant of the order 0.1; k_f = shear unbiased jump frequency of a flow defect; γ_0 = shear strain per jump of a defect; v_0 = volume of a defect; Ω = atomic volume. (Note: the quantity c_f used here is related to the n_f used by Spaepen as $c_f = n_f\Omega$.)

For k_f we write

$$k_f = \nu_0 \exp(-Q/RT) \tag{2}$$

where ν_0 is expected to be about the Debye frequency ν_D and Q is an activation energy.

During structural relaxation the excess free volume anneals out. This can be described by the annihilation of excess flow defects at special sites, called "relaxation sites" with concentration c_r. The annihilation rate of flow defects is then

$$\dot{c}_f = -k_r c_f c_r \tag{3}$$

where k_r = jump frequency of the annihilation process. As there is no *a priori* reason why this frequency should differ from the jump frequency of the flow defects, we put

$$k_r = k_f. \tag{4}$$

Further, as it has been assumed initially [5] and supported by experimental evidence later on [6] by Spaepen and coworkers, the annihilation of flow defects is a bimolecular process, i.e.

$$c_r = \beta c_f \tag{5}$$

where β is a constant.

Then from equation (3), (4) and (5) we have

$$\dot{c}_f = -k_f \beta c_f^2 \tag{6}$$

and this equation has the solution

$$c_f^{-1} - c_{f_0}^{-1} = C_0 t \exp(-Q/RT) \tag{7}$$

with $C_0 = \beta\nu_0$.

The available experimental data of the quantity $\gamma_0 v_0$ has been extensively discussed by Taub [7]. From this data it will be shown further on that in a certain temperature range (range I) below the glass temperature, the temperature dependence of $\gamma_0 v_0$ can be represented by

$$\gamma_0 v_0 = A \exp(-Q_s/RT). \tag{8}$$

Substitution of (2) and (8) in (1) yields, for range I

$$\eta = T.c_f^{-1} C \exp(Q_\eta/RT) \tag{9}$$

with $Q_\eta = Q + 2Q_s$ and

$$C = \frac{k\Omega}{\nu_0 A^2}. \tag{10}$$

In the temperature range below that for which equation (8) is valid (range II), $\gamma_0 v_0$ becomes nearly independent of temperature, so that here we have

$$\eta \sim T c_f^{-1} \exp(Q/RT). \tag{11}$$

Finally it follows from (7) and (9)

$$\dot{\eta}/T = CC_0 \exp(2Q_s/RT) \tag{12}$$

in range I.

It is emphasized that the foregoing expressions, in particular equation (7), have been derived under the assumption that the structural relaxation process considered is the annealing out of free volume, i.e. TSRO. In a previous study [4] on structural relaxation in $Fe_{40}Ni_{40}B_{20}$ it has been made plausible that this is the case in the later stages of structural relaxation, in the temperature range preceding crystallization. We shall identify this stage with range I, mentioned before. In the lower temperature range (II)

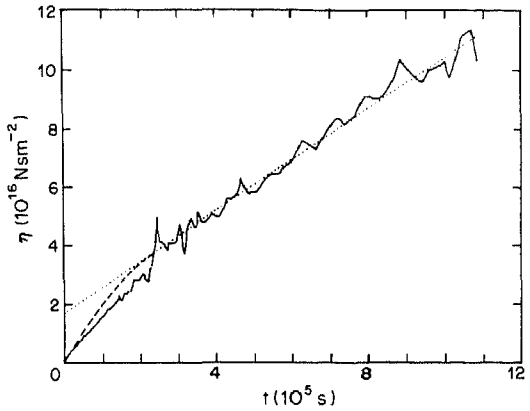

Fig. 1. Isothermal variation of viscosity at 523 K in as-quenched specimen A. Dashed line: after correction for the anelastic strain rate (Section 4.3).

chemical ordering (CSRO) is the important relaxation process, as indicated by the results of Ref. [4].

In the following the theory is tested experimentally by viscosity measurements on FeNiB in the following ways:

1. An attempt is made to discriminate the contributions of CSRO and TSRO to the viscosity change in the boundary range between I and II.
2. Combination of equations (1), (7) and (12) shows that η varies linearly with time in range I. This has been observed by several investigators in various amorphous systems (e.g. [8–10]). So from $\eta(t)$ measurements the kinetics of flow defects can be studied, which, by use of (7), should yield Q.
3. From (12) it is seen that, in range I, a plot of $\ln(\dot{\eta}/T)$ vs 1/T should yield a straight line, which provides both Q_s and CC_0. The Q_s obtained in this way can be compared with the value found from equation (8), describing the temperature dependence of $\gamma_0 v_0$.
4. In a so called "isoconfigurational" experiment, the viscosity is measured as a function of temperature at constant flow defect concentration c_f. Then it follows from (9) and (11) that a plot of $\ln \eta/T$ vs $1/T$ should yield $Q + 2Q_s$ and Q, respectively, in ranges I and II. As both Q and Q_s were determined previously, in this way the model is checked on internal consistency.
5. From (9) we have, in range I:

$$\eta c_f . T^{-1} = C \exp(Q + 2Q_s)/RT. \qquad (13)$$

From the thermal history of each specimen, c_f can now be calculated using the kinetics determined (1 sub 2). Together with the measured η and T values, (13) predicts that all the data in range I can be brought together in one "master plot", where $\ln(\eta c_f T^{-1})$ is plotted vs $1/T$. This should yield a single straight line with slope $(Q + 2Q_s)/R$ and intercept C. The value of C is compared with equation (10).

3. EXPERIMENTAL RESULTS AND ANALYSIS

The experimental set-up was described in a previous paper [11]. The material used was $Fe_{40}Ni_{40}B_{20}$ (Vitrovac 040) supplied by Vacuumschmelze. The ribbons had cross-sectional dimensions of $2.78 \times 0.033 \times mm^3$ and were tested in tension with a gage length, as defined by the hot zone, of 200 mm. The viscosity measurements were performed with a constant stress of 110 MPa. It was verified that this stress is in the range where a linear stress–strain rate relation exists. All the data come from two specimens, A and B which were subjected to different multistage thermal treatments.

3.1. Specimen A

The as-quenched specimen A was first annealed at 523 K, during which the viscosity was measured as a function of time. The result is shown in Fig. 1. Subsequently the same specimen was held at 543, 563 and 583 K and the resulting $\eta(t)$ plots are presented in Fig. 2.

The latter $\eta(t)$ relations are all linear, in contrast to the result of Fig. 1, where $\eta(t)$ only becomes linear after an initial transient of about 3.10^5 s. This period corresponds to the time which, according to a previous study [4], is necessary for the completion of CSRO in this material. It is concluded that the initial part of the curve in Fig. 1 represents viscosity changes to CSRO. (This is discussed further in Section 4.3, where the role of anelasticity is also taken into account.) This also means that the temperature of 523 K is in the boundary region between ranges I and II mentioned in Section 2. In Fig. 2 no effect of CSRO is visible. This can be ascribed to two reasons. First, the kinetics of CSRO becomes much faster at higher temperatures (roughly by a factor of 10 for $\Delta T = 20$ K). Second the change in CSRO from the as-quenched state to the equilibrium state at 523 K is much larger than the change in equilibrium CSRO between 523 and 543 K, etc. It is concluded

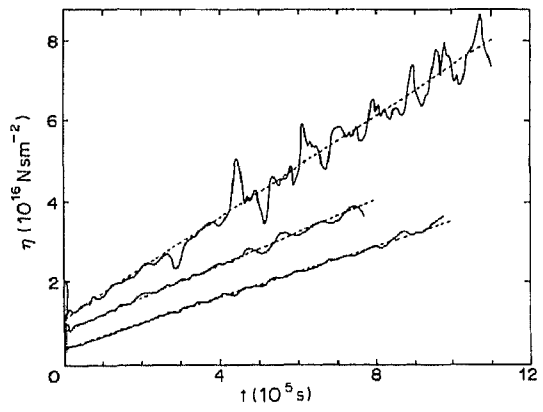

Fig. 2. Isothermal variation of viscosity during annealing of specimen A after Fig. 1 at 543, 563 and 583K respectively.

Table 1. Activation energy of flow defect annihilation

Specimen	T_1(K)	T_2(K)	$t_1(10^4\,s)$	$t_2(10^4\,s)$	f_1	f_2	$Q\left(\frac{kJ}{mol}\right)$
A	523	543	111	112	6.9	7.8	245
A	543	563	112	80	7.8	5.45	250
A	563	583	80	101	5.45	9.2	283
B	550	570.7	63	58.3	7.2	6.4	241
B	570.7	591.4	58.3	33.2	6.4	3.85	241

that in the measurements of Fig. 2 CSRO is in equilibrium almost from the beginning.

As pointed out in Section 2, the linear increase of η with time is in accordance with the kinetics of flow defect motion as described by the free volume model [equation (7)]. From the data the activation energy Q can be determined in the following way.

When at a temperature T_1 during a time t_1 the viscosity changes from an initial value η_{1i} to a final value η_{1f}, we have from (1) and (7)

$$f_1 = \frac{\eta_{1f}}{\eta_{1i}} = \frac{(c_f)_i}{(c_f)_f} = 1 + (c_f)_i . C_0 t_1 \exp\left(-\frac{Q}{RT_1}\right). \qquad (14)$$

After this, the temperature is increased to T_2, where during a time t_2 η changes from η_{2i} to η_{2f}. Realizing that $(c_f)_f = (c_f)_i = (c_f)_i . f_1^{-1}$, we have

$$f_2 = \frac{\eta_{2f}}{\eta_{2i}} = \frac{(c_f)_i}{(c_f)_f} = 1 + f_1^{-1}(c_f)_i . C_0 t_2 \exp\left(-\frac{Q}{RT_2}\right). \qquad (15)$$

From (14) and (15) it follows

$$f_1 . \frac{f_2 - 1}{f_1 - 1} = \frac{t_2}{t_1} \exp\left\{\frac{Q}{R}\left(\frac{1}{T_1} - \frac{1}{T_2}\right)\right\}. \qquad (16)$$

For every set of temperatures (T_1, T_2) and times (t_1, t_2), f_1 and f_2 can be determined and Q follows from (16). The results (two of which are obtained from specimen B) are given in Table 1. The average value of Q is 252 kJ/mol, with a standard deviation of 7 kJ/mol. This is very close to the result $Q = 250$ kJ/mol, obtained from our previous analysis [4]. It was argued there that the constant C_0 cannot be determined in an absolute way: it depends on the value of $x = v_f/\gamma v^*$ in the as-quenched state, which is not known.

It was shown that, when one of the two quantities is chosen, the flow defect kinetics can describe the length and modulus changes in range I in a satisfactory way. The same is done here and in principle the same choice is made as in Ref. [4], with two modifications. First, it was discovered after publication of Ref. [4], that in the length measurements a small error had been made in the temperature determination, which had to be corrected for. Reanalysis of the data showed that, for the same $x_{aq} = 0.0753$, C_0 had to be modified from $3.39 . 10^{25}\,s^{-1}$ to $1.63 . 10^{25}\,s^{-1}$. The results of the analysis in Ref. [4] remain largely unaffected; only the times for attaining complete CSRO given in Table 3 of the paper have to be multiplied by about a factor of 2. Second, the fit of the present data to equation (7) improves by a slight adjustment of $x_{aq} = 0.079$ instead of 0.0753. So the flow defect kinetics can be described here with equation (7) and the parameter values $Q = 250$ kJ/mol; $C_0 = 1.63 . 10^{25}\,s^{-1}$; $x_{aq} = 0.079$. Finally, the results of specimen A shown in Figs 1 and 2 can be used to construct a plot as suggested by equation (12): $\ln(\dot{\eta}T^{-1})$ vs T^{-1}. This is done in Fig. 3. The result is a straight line of the form

$$\dot{\eta}T^{-1} = 700 \exp(54{,}000/RT)$$

which yields $CC_0 = 700\,Nm^2K^{-1}$ and $2Q_s = 54$ kJ/mol. From the value of C_0 given before we have $C = 4.29 . 10^{-23}\,Nsm^{-2}K^{-1}$.

The results of the analysis of the specimen A data can be summarized as follows:

1. Apart from the initial part at the lowest temperature (523 K) the observed changes in η are in agreement with the free volume model of structural relaxation as described by equations (1), (7) and (12). The parameters found from the analysis are: $Q = 250$ kJ/mol; $2Q_s = 54$ kJ/mol; $CC_0 = 700\,Nm^{-2}K^{-1}$. Taking $C_0 = 1.63 . 10^{25}\,s^{-1}$, $C = 4.29 . 10^{-23}\,Nsm^{-2}K^{-1}$.
2. The initial transient in $\eta(t)$ at 523 K (Fig. 1) can be ascribed to CSRO, in accordance with earlier results [4]. This temperature is roughly the boundary between ranges I and II where TSRO resp. CSRO are the dominating structural relaxation processes.

3.2. *Specimen B*

This specimen was first annealed for 10^6 s at 470 K (measurement 1, table 2). After that the viscosity

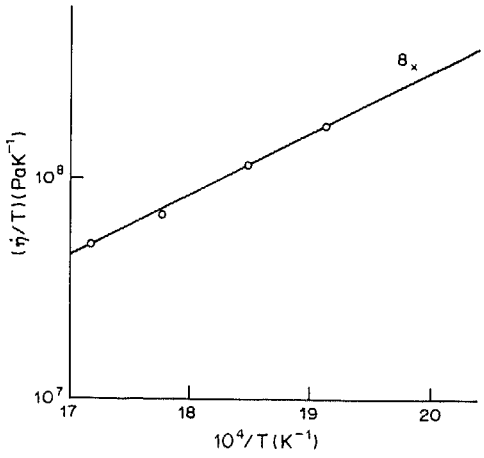

Fig. 3. Log $\dot{\eta}/T$ for specimen A. × see text (Section 4.3.)

Table 2. Viscosity of specimen B and calculated flow defect concentration

NR	T(K)	$t(10^4$ s)	η (10^{16} Nsm^{-2})	$c_f(10^{-8})$	NR	T(K)	$t(10^4$ s)	η (10^{16} Nsm^{-2})	$c_f(10^{-8})$
1	470.3	100	—	318	20	550.0	63	3.4	4.75
2	455.0	10.1	~400	318	21	533.3	14.9	36	4.59
3	463.0	5.76	77	318	22	541	7.2	11.3	4.34
4	470.3	8.0	43	318	23	550.0	2.3	3.5	4.34
5	478.6	1.19	21	318	24	522.4	23.3	~130	4.16
6	490.0	0.79	5.1	318	25	560.4	1.76	1.14	3.93
7	470.3	5.58	51	318	26i	570.7	—	0.38	3.93
8i	502.4	—	1.13	318					
8	502.4	35.1	7.2	270	26	570.7	58.3	2.3	0.68
9	478.6	7.31	133	270	27	560.4	8.46	8.4	0.65
10	490.0	5.87	27.5	268	28	550.0	23.5	28.7	0.62
11	517.1	0.43	1.63	265	29	581.0	1.76	0.85	0.59
12i	533.3	—	0.31	265	30i	591.4	—	0.31	0.59
12	533.3	41.7	3.4	40.6	30	591.4	33.2	1.2	0.164
13	478.6	8.64	—	40.6	31	583.1	2.7	2.9	0.157
14	502.4	16.3	94	40.2	32	574.9	5.3	8.1	0.153
15	517.1	2.27	12.6	39.8	33	601.4	2.35	0.46	0.138
16	490.0	22.2	~410	39.8					
17	533.3	1.01	2.6	39.0					
18	544.8	0.79	0.69	37.0					
19	533.3	6.4	4.1	33.1					
20i	550.0	—	0.5	33.1					

was measured at the temperatures and during the times indicated in Table 2 (measurements 2–8i). The measuring time was chosen as short as possible in order to avoid appreciable structural relaxation (which would increase η) and long enough to allow a reasonably accurate ($\pm 10\%$) viscosity measurement. In other words: the intention of series 2–8i was to produce an isoconfigurational set of data. After 8i, the specimen was kept for a long time at the same temperature, during which the viscosity increases due to structural relaxation. Then a second isoconfigurational set was carried out (8–12i) and so on. In this way 6 isoconfigurational sets were obtained. The results are given in table 2 and represented, as $\log(\eta T^{-1})$ vs T^{-1} in Figs 4 and 5.

The lines in Fig. 4 lie in temperature range II. According to equation (11) the expected activation energy is $Q = 250$ kJ/mol, as observed in specimen A and in previous work [4]. The values obtained are indicated in Fig. 4: 235, 243 and 247 kJ/mol, in good agreement with the prediction. The lines in Fig. 5 fall in range I. The activation energy expected here is, according to (9), $Q_\eta = Q + 2Q_s = 304$ kJ/mol, as found earlier in this section. The observed values are 304, 302 and 315 kJ/mol, again in good agreement with the expectation.

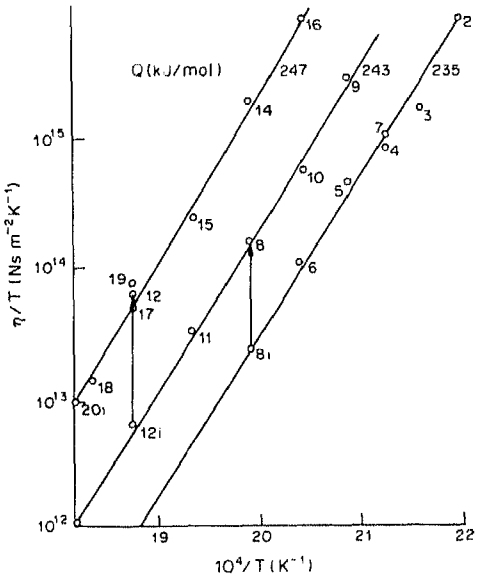

Fig. 4. η/T vs $1/T$ for specimen B, measurements 2–20i (Table 2).

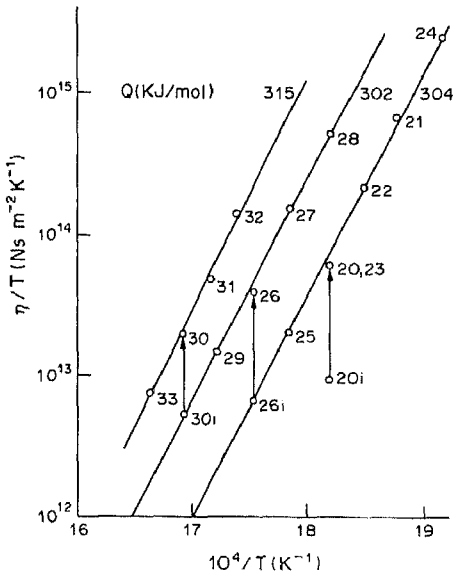

Fig. 5. η/T vs $1/T$ for specimen B, measurements 20–33 (Table 2).

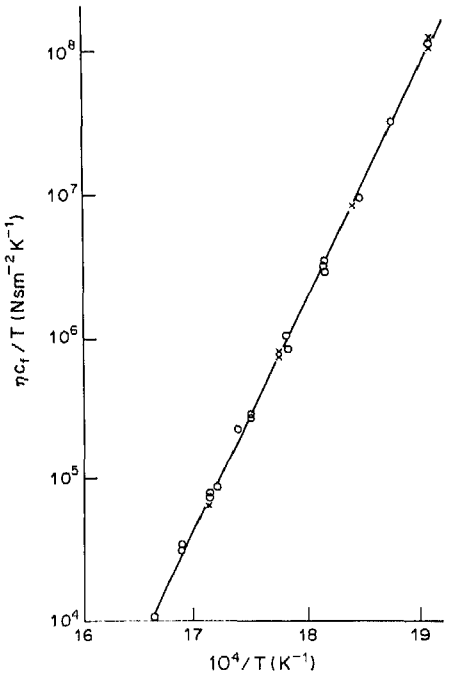

Fig. 6. Log($\eta c_f T^{-1}$) vs $1/T$. × specimen A; ○ specimen B, measurements 20–33.

Finally, as the parameters Q and C_0 describing the kinetics of flow defect annihilation through equation (7), are known, the flow defect concentration c_f can be calculated for all the data of specimens A and B. The results are given in Table 2 for the data of specimen B. In the high temperature range I, equation (13) should be valid. As suggested by this equation, the quantity $\ln(\eta c_f T^{-1})$ is plotted vs T^{-1} in Fig. 6 for the data of specimen A and measurements 20–33 (Table 2) of specimen B. The drawn straight line is the representation of $\eta c_f T^{-1} = C \exp(Q_\eta/RT)$, with $C = 4.29.10^{-23}$ Nsm^{-2}K^{-1} and $Q_\eta = 304$ kJ/mol, as obtained earlier. It is concluded that all the data are well described by a single straight line over 4 orders of magnitude in $\eta c_f T^{-1}$ and that the slope and intercept of this line are in agreement with the prediction.

The same procedure has been applied to the data in range II (specimen B, measurements 2–19). The results are shown in Fig. 7. The straight line on the left hand side is the same one as in Fig. 6, representing the data in range I. It is clear that this time the data do not come together on a straight line. The Q values computed from the slopes of the 3 straight lines, which correspond to those in Fig. 4, are indicated in the figure. They are again about 250 kJ/mol. The Q values are slightly different from those in Fig. 4, because the straight lines in that figure are, strictly speaking, not isoconfigurationals. This is due to the fact that (see Table 2) within one "isoconfigurational" set the values of c_f may vary by 10–20%. This difficulty is removed by plotting the quantity $\eta c_f T^{-1}$ as done in Figs 6 and 7.

The existence of two temperature ranges is clearly demonstrated by figs 6 and 7. In the high temperature range I (520–600 K) the structural relaxation can be described by free volume annihilation (TSRO) only. When the decrease of free volume is accounted for by computing c_f from (7), all the data in range I constitute a single straight line in the plot of Fig. 6. The slope of the line yields $Q_\eta = 304$ kJ/mol, which is attributed to a contribution of two parts: $Q = 250$ kJ/mol due to the annihilation of flow defects and $2Q_s = 54$ kJ/mol from the temperature dependence of the shear volume v_0. In the lower temperature range II ($T < 520$ K), after correction for the decrease of free volume, major changes in viscosity remain visible (Fig. 7). These must be attributed to chemical ordering (CSRO), which continuously increases during the series 2–20i of specimen B. The final points of this series (17–20i) approach the range I line rather closely, indicating that equilibrium CSRO has now been attained. This is in agreement with the data of Fig. 1, as discussed earlier, and with the results of the analysis of elastic modulus and length measurements presented in a previous paper [4].

4. DISCUSSION

The following points need some further discussion.

4.1. *Temperature dependence of* $\gamma_0 v_0$

It was first noted by Taub and Spaepen [8] that the activation energy of the viscosity Q_η in $Pd_{80}Si_{20}$ is larger (by 31 kJ/mol) than the activation energy Q of the annealing out of the flow defects. Our measurements confirm this observation for FeNiB: $Q_\eta = 304$ kJ/mol and $Q = 250$ kJ/mol respectively. In Section 2 this was tentatively ascribed to the temperature dependence of $\gamma_0 v_0$ in equation (1). It was proposed

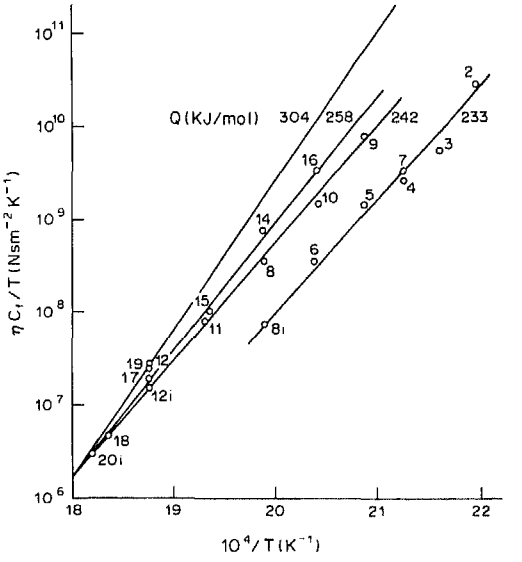

Fig. 7. Log($\eta c_f T^{-1}$) vs $1/T$ for specimen B, measurements 2–20i.

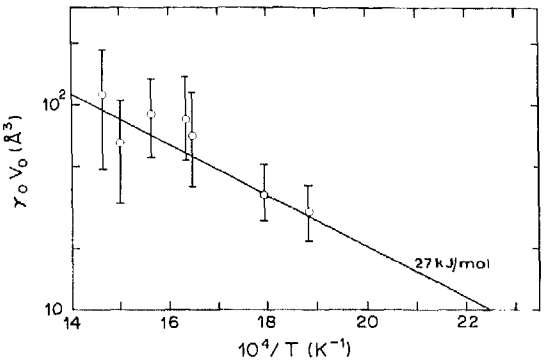

Fig. 8. Log($\gamma_0 v_0$) vs $1/T$ for Metglas 2826. Data from Taub [7].

to write this, in range I, in an exponential form [equation (8)]. This needs some justification.

In Ref. [7], Fig. 11, Taub presents $\gamma_0 v_0$ as a function of temperature for three amorphous alloys. Qualitatively the curves all have the same shape: $\gamma_0 v_0$ is only weakly temperature dependent at low temperatures and increases at higher temperatures (identified by us as range I). Unfortunately, no data are available for FeNiB. Therefore we use the data of FeNiPB (Meiglas 2826) which in many respects behaves as FeNiB. This data is replotted in Fig. 8 as $\log(\gamma_0 v_0)$ vs T^{-1}. The drawn line is constructed according to equation (8), with $Q_s = 27$ kJ/mol and $A = 1.3.10^{-26}$ m^3. Although the inaccuracy of the data does not permit an accurate determination of Q_s, the proposed relationship seems to be acceptable.

The question remains why $\gamma_0 v_0(T)$ behaves in this way. It should be remembered that, in our interpretation, in range I the chemical order comes to equilibrium at all temperatures in a short time. This means that with increasing temperature, CSRO decreases, i.e. the structure becomes less tightly bound, which could give rise to an increase of the volume v_0 participating in a shear jump. In region I, roughly between 520 and 600 K, this would give rise to an increase in v_0 by a factor of 2, which is not *a priori* unreasonable.

4.2. *The attempt frequency* ν_0

From (10), with $C = 4.29.10^{-23}$ Nsm^{-2} K^{-1}; $\Omega = 11.10^{-30}$ m^3 (the mean value of Ω in crystalline Fe and Ni); $A = 1.3.10^{-26}$ m^3, we find $\nu_0 = 2.10^{22}$ s^{-1}. In comparison with the expected Debye frequency $\nu_D \sim 10^{13}$ s^{-1} this seems an unphysically high value. This is, however, not the first time this problem is met. It seems more or less systematical that, whenever in the literature it was tried to obtained ν_0 from the data, values between 10^{19} and 10^{25} s^{-1} were reported (see e.g. [3, 8, 12]). Perhaps the most direct evidence comes from internal friction measurements by Berry [12] on $Fe_{80}B_{20}$ who finds $\nu_0 = 10^{25}$ s^{-1}. Berry also suggested an explanation for this result: if the activation energy for flow defect motion should depend linearly on temperature: $Q = Q_0(1 - \alpha T)$ (α is a constant), then $\nu = \nu_D \exp(\alpha Q_0/R) \exp(-Q_0/RT) = \nu_0 \exp(-Q/RT)$ with $\nu_0 = \nu_D \exp(\alpha Q_0/R)$.

Taking $\alpha = 7.10^{-4}$; $Q_0 = 250$ kJ/mol and $\nu_D = 10^{13}$ s^{-1} we have $\nu_0 = 10^{22}$ s^{-1}. The suggested explanation might be correct, but has to be proved as yet.

4.3. *Linear and non-linear* $\eta(t)$ *relations*

In the result of the as-quenched specimen A, shown in Fig. 1, $\eta(t)$ becomes linear only after an initial transient. The linear part, as shown before, is in agreement with a TSRO-interpretation. It is therefore tempting, and in accordance with the modulus data of Ref. [4], to ascribe the transient to an increase of η due to CSRO. Before this can be done with some confidence, first the role of anelasticity to the observed effects will be discussed.

The transient has been reported in the literature several times (e.g. [7]) and related to an anelastic contribution to the relaxation. In order to verify this, the experiment of Fig. 1 was repeated during the first $2.4 \cdot 10^5$ s, after which the load was removed and the anelastic strain was measured. The result is shown in Fig. 9, giving $\varepsilon(t)$ before and after unloading. The dotted line is the calculated contribution of TSRO to the strain. The remaining $\varepsilon(t)$ after unloading is interpreted as an anelastic effect. If this is correct, this part of the strain (with reversed sign) is also a contribution to $\varepsilon(t)$ in the loaded condition and a correction in η due to anelasticity can be calculated. The result is shown in Fig. 1 as a dashed line. It is seen that the transient is only partly accounted for by anelasticity and we propose that the remaining part is due to CSRO. The relaxation time of about 2.10^5 s is in accordance with the value found from the modulus measurements [4], which was ascribed to CSRO. It is noted that the relaxation time of the anelastic effect is about the same. This seems satisfactory, because the interpretation of anelasticity is

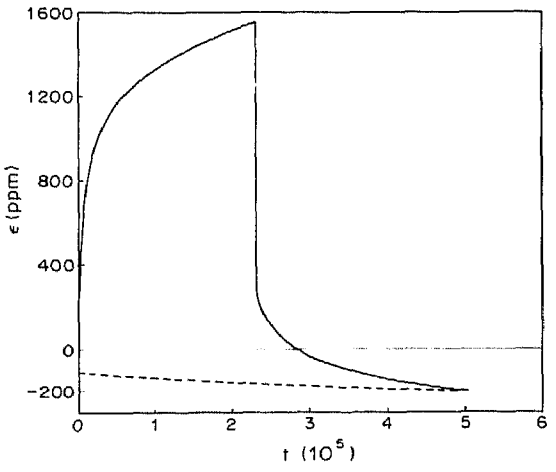

Fig. 9. Strain vs time at 523 K of a loaded specimen, followed by unloading. Dotted line: calculated free volume contribution.

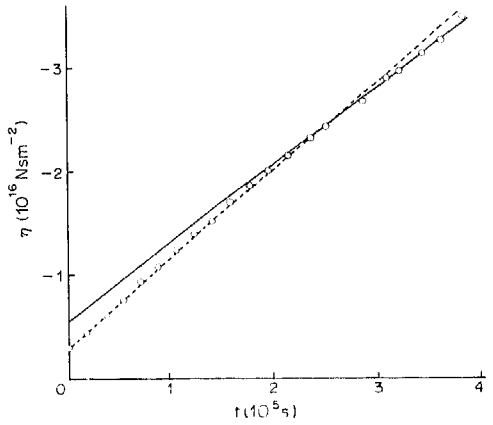

Fig. 10. Isothermal variation of viscosity at 533.3 K, specimen B, measurement 12i–12. Drawn line: calculated, Dashed line: see text. (section 4.3).

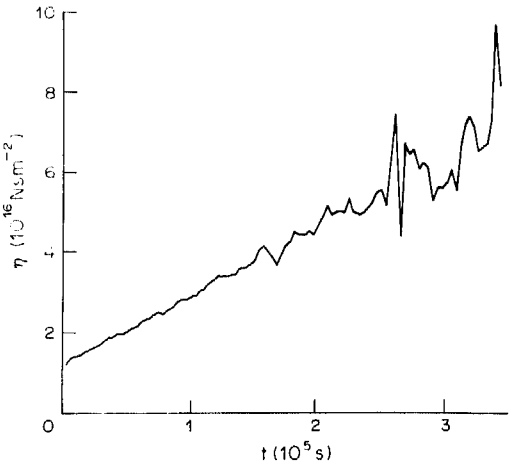

Fig. 11. Isothermal variation of viscosity at 502.4 K, specimen B, measurement 8i–8.

that it is an ordering process also ("stress induced ordering").

An intermediate case between Figs 1 and 2 is shown in Fig. 10. This is measurement 12i–12 of specimen B at 533 K, just between the temperatures of Figs 1 and 2. The drawn line was calculated from equations (7) and (9) with the parameters given before. With respect to this line the data points show a small initial transient, with a time constant about a factor 2 smaller than in Fig. 1. After about $1.5 \cdot 10^5$ s equilibrium CSRO has been attained, and further changes in η are due to TSRO and fit the drawn line calculated on this basis. (This also explains why in Fig. 7 point 12 falls on the equilibrium line whereas point 12i does not.) However, an investigator who was not intentionally looking for the effect could easily have drawn the dashed line in Fig. 10 through the data points and have concluded to a linear $\eta(t)$ relation from the beginning. On the other hand, in Fig. 11 $\eta(t)$ is represented for measurement 8i–8 of specimen B at a temperature of 502.4 K which is 20 K lower than the temperature of Fig. 1. Again the observed $\eta(t)$ is linear. However, the value of η at equilibrium CSRO, calculated from (9), is about 3.10^{17} Nsm^{-2}, which is larger by a factor of 4 than η at the end of the anneal in Fig. 11. The estimated time for the completion of CSRO in this case is larger by a factor of 10 than at 523 K (Fig. 1), i.e. about 2.10^6 s. This is about 10 times the measuring time in Fig. 11. So in our interpretation, in Fig. 11 equilibrium CSRO is far from being attained. The increase of η in this measurement is due to increasing CSRO and in the (relatively short) time of the measurement it is linear in time. This is in agreement with the fact that the slope of $\eta(t)$ in this case does not fit well in the data of Fig. 3 (indicated with a cross), which were taken in range I. The foregoing may demonstrate why it is difficult to find a result as in Fig. 1, which shows the transition from CSRO to TSRO directly. The fact that we were guided to find the appropriate temperature by our previous analysis of completely different data [4], corroborates the internal consistency of the picture presented.

4.4. High temperature limit: crystallization

The temperature in range I where structural relaxation experiments as described can be carried out is limited by the onset of crystallization. This is about 600 K, as demonstrated in Fig. 12, where the result of the final experiment on specimen A is shown: $\eta(t)$ at 603 K. It shows a large, non-linear increase of viscosity, due to crystallization.

4.5. Dependence of physical properties on free volume

In the free volume model of structural relaxation the viscosity is an unique property, because it depends on the free volume v_f through the factor $c_f^{-1} = \exp(x^{-1})$ where $x = v_f/\gamma v^*$. This yields, by equations (1) and (7), the linear increase of η with time. Changes in other physical properties like length,

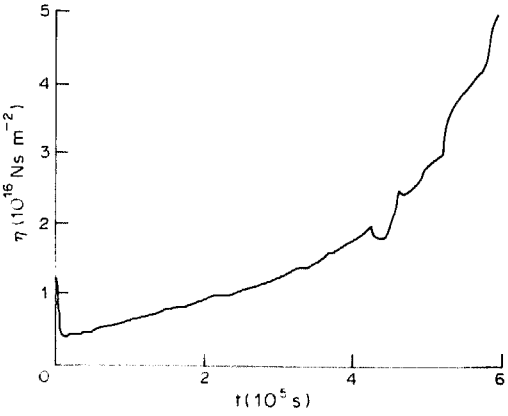

Fig. 12. Isothermal variation of viscosity at 603 K, specimen A, after Fig. 2.

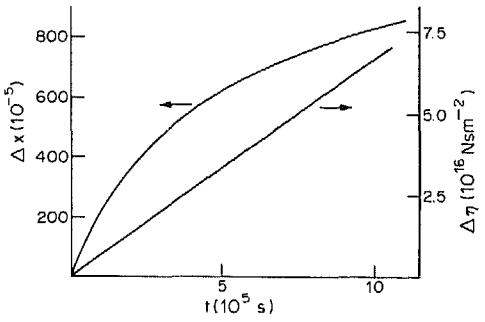

Fig. 13. Different behaviour of viscosity and free volume upon isothermal annealing.

elastic moduli, resistivity, are (in the simplest case) proportional to changes in the free volume itself. This gives rise to a completely different property vs time relation which is often, but not completely correctly, referred to as a linear property vs log t relation. The difference is demonstrated in Fig. 13. The straight line is the $\eta(t)$ result of specimen A at 543 K earlier presented in the Fig. 2. The second curve represents the accompanying change in free volume Δx, as calculated from (7). The fact that in range I the observed viscosity changes reported in this paper and the observed changes in length and Young's modulus reported earlier [4] can be described by the same formalism with the same parameters, in our opinion strongly supports the interpretation presented.

4.6. Strain rate correction due to structural relaxation

In measurements as those in Figs 1 and 2 the observed strain rates from which η was determined are, in principle, due to two causes: (1) the applied stress; (2) structural relaxation itself, which gives rise to a negative strain rate (contraction). In a previous paper [13] it was shown that the experimental strain rates have to be corrected for the effect (2) in order to obtain correct η values. The importance of the correction becomes larger with decreasing applied stress. In the present experiments we have carried out the correction for part of the data and found only a minor influence at the particular stress used in this study. As the correction is a very tedious affair, it was decided to omit it further. So all the viscosity data presented were uncorrected for the structural relaxation effect.

4.7. Comparison with other investigations

In the foregoing our results were occasionally discussed with reference to the results of other investigators, in particular those of Spaepen and coworkers. In general, there is a broad correspondence between Spaepen's results, mainly on PdSi(Cu) alloys and our results on FeNiB. In one respect they clearly differ: the "isoconfigurationals" in the low temperature range, as presented in Fig. 4, are all reasonably straight lines. In a recent report by Tsao and Spaepen [6] analogous data for PdSiCu were presented which showed marked deviations from a linear log η vs T^{-1} relation. At low temperatures the curves flatten off. This led the authors to the conclusion that "isoconfigurational flow is essentially non-Arrhenian". Although we have no clear explanation for this observation, it is noted that the deviations occur in what we have called range II, the temperature range where CSRO is the predominant process. Moreover, the deviations shift to higher temperatures when the specimens had been kept for a longer time at higher temperatures. It has been suggested [3] that the rate of chemical ordering is dependent on the amount of free volume through the term $\exp(-x^{-1})$ and therefore slows down with decreasing free volume. It is possible that the state of CSRO along an "isoconfigurational", which is in equilibrium at the higher temperatures, becomes not well defined and history dependent in the lower temperature range. This could also give rise to the "crossing over" of the various isoconfigurationals in Fig. 3 of Ref. [6]. At the moment, however, we have not enough data to work out these suggestions in more detail. Another discrepancy with Spaepen and coworkers is in the interpretation of the temperature dependence of η as described by equation (9). In our interpretation the observed activation energy Q_η is essentially, apart from the relatively small correction term $2Q_s$, the activation energy of flow defect motion $Q = 250$ kJ/mol, which is also the activation energy of flow defect annihilation. This was expressed by equation (4), stating that the jump frequency of flow defect annihilation is the same as that of flow defect motion. In other words: the flow defects annihilate by moving, just as vacancies in crystalline material. To us this seems to be the most simple and logical assumption and the present data can be consistently analyzed in this way. In Spaepen's opinion [6], the activation energy of flow defect motion is rather small (<50 kJ/mol) and this is based mainly on the flattening off of the log η vs T^{-1} curves at low temperatures discussed before. In order to explain the high value of Q_η in range I, Spaepen introduces a reversible flow defect concentration in this temperature range, which should be due to a reversible redistribution of free volume. In this model $k_f \neq k_r$ and the annihilation should be governed by an activation energy much higher than that of motion of the flow defects. To us this seems an unsatisfactory feature of the model. Moreover, it was argued by Tsao and Spaepen [6] that the critical free volume fluctuation v^* is about 6% of an atomic volume. This would mean that the "vacancies" in amorphous alloys are very much smaller than in crystalline materials. As in crystalline Fe and Ni the activation energy of vacancy motion is about 100 kJ/mol, it is not well understandable why this should be considerably smaller in amorphous alloys on FeNi basis. Intuitively the reverse should be expected. Finally, as was noted earlier by Van den Beukel and Radelaar

[3], the two interpretations lead to a different description of $\eta(T)$ in *equilibrium* near the glass temperature. In Spaepen's interpretation, the temperature dependence in this range is governed only by the term c_f^{-1} in equation (9) leading to the well known Fulcher–Vogel expression $\eta \sim \exp(B/T - T_0)$. In our idea the exponential term $\exp(Q_\eta/RT)$ in (9) describing the energy barrier for flow defect motion, should also be maintained. This leads to an expression of the form $\eta \sim \exp(B/T - T_0)\exp(Q_\eta/RT)$, a so called "hybrid" equation. Unfortunately, as was first shown by Van den Beukel and Radelaar [3] and later on by Tsao and Spaepen [6], the scarce experimental data of $\eta(T)$ in equilibrium do not permit, within the experimental accuracy, to decide between the two expressions. In conclusion, it seems desirable to extend the investigation of the $\eta(T)$ behaviour in the low temperature range of PdSiCu and possibly other systems, keeping in mind that the kinetics of chemical ordering may play an important role.

5. CONCLUSIONS

1. In the analysis of observed viscosity changes during structural relaxation in $Fe_{40}Ni_{40}B_{20}$ two regimes can be distinguished: (a) the high temperature range I ($\sim$520–600 K) where the data can be described consistently in terms of the annealing out of flow defects (TSRO); (b) the low temperature range II ($T < 520$ K) where chemical ordering (CSRO) is the dominating process.

2. In range I it was found that:

(a) The activation energy for annihilation of flow defects $Q = 250$ kJ/mol.

(b) After correction for the decay of flow defects, all the viscosity data fall on a single straight line in a log η vs T^{-1} plot. The corresponding activation energy is $Q_\eta = 304$ kJ/mol.

(c) The difference between Q_η and Q can be ascribed to a reversible temperature dependence of the shear volume v_0, probably due to changes in equilibrium CSRO.

3. In a narrow transition range between I and II the contributions of CSRO and TSRO to the increase in viscosity can be clearly distinguished experimentally.

4. In range II, isoconfigurational plots of ln η vs T^{-1} yield an activation energy of about 250 kJ/mol, close to the value found for the annihilation of flow defects. There is no need to distinguish between the jump rate of flow defect motion and annihilation. The increase of viscosity observed in this range cannot be ascribed to flow defect annihilation and is ascribed to an increase of chemical order (CSRO).

Acknowledgement—This work was performed as a part of the research program of the "Stichting voor Fundamenteel Onderzoek der Materie".

REFERENCES

1. T. Egami, *Ann. N.Y. Acad. Sci.* **371,** 238 (1981).
2. F. Spaepen, *Acta metall.* **25,** 407 (1977).
3. A van den Beukel and S. Radelaar, *Acta metall.* **31,** 419 (1983).
4. A. van den Beukel, S. van der Zwaag and A. L. Mulder, *Acta metall.* **32,** 1895 (1984).
5. F. Spaepen, in *Les Houches Lectures XXV* (edited by J. J. Poirier and M. Kleman), North Holland, Amsterdam (1981).
6. S. S. Tsao and F. Spaepen, Office of Naval Research, Tech. Rep. No. 25 (1984).
7. A. I. Taub, *Acta metall.* **30,** 2117, 2129 (1985).
8. A. I. Taub and F. Spaepen, *Acta metall.* **28,** 1781 (1980).
9. A. I. Taub and F. Spaepen, *Scripta metall.* **14,** 1197 (1980).
10. A. I. Taub and F. E. Luborsky, *Acta metall.* **29,** 1939 (1981).
11. A. L. Mulder, S. van der Zwaag, E. Huizer and A. van den Beukel, *Scripta metall.* **18,** 515 (1984).
12. B. S. Berry, *Scripta metall.* **16,** 1407 (1982).
13. E. Huizer, A. L. Mulder and A. van den Beukel, *Acta metall.* **34,** 493 (1986).